



Applications of TDLAS based multi-species hydrocarbon measurement using a wide scanning range DFG laser

Qiming Wang^a, Zhenzhen Wang^{a,b}, Takahiro Kamimoto^a, Yoshihiro Deguchi^{a,b,*}, Du Wen^b, Daichi Takahara^a

^a Graduate School of Advanced Technology and Science, Tokushima University, Tokushima, 770-8501, Japan

^b State Key Laboratory of Multiphase Flow in Power Engineering, Xi'an Jiaotong University, Xi'an, 710049, China

ARTICLE INFO

Keywords:

Hydrocarbon measurement
Tunable diode laser absorption spectroscopy (TDLAS)
Difference frequency generation (DFG)
Coal pyrolysis
Engine exhaust

ABSTRACT

Tunable diode laser absorption spectroscopy (TDLAS) is a widely used hydrocarbon gas sensing method in many fields. However, the short scanning range limits its application where multi-species detection is necessary. In this paper, a laser system based on TDLAS using a difference frequency generation laser was applied for the investigation of the hydrocarbon gases produced in the coal pyrolysis process and engine exhaust. The coal sample was heated up to 623 K and the recorded spectra were analyzed by the comparison with the pure hydrocarbon spectra database. A least-squares fitting was performed to quantitatively determine the concentration of each component of the mixture. Totally nine different hydrocarbons were identified and the R^2 values close to 1 indicate that the variance between measured and fitted data was small. The spectra of engine exhaust were recorded and analyzed using the same method. Hydrocarbon from C_3 – C_8 and a small amount of methane and ethene were identified. The concentration variation with time was observed.

1. Introduction

As a common chemical compound, the detection of hydrocarbon is widely discussed from fundamental research to industrial application. In the coal industry, pyrolysis (or devolatilization) is an important initial step for most coal conversion processes, such as combustion, gasification and liquefaction [1]. The volatiles and tars released during this step account for up to 70% of the total weight loss [2–4]. As a major component in the gaseous product, it is important to explore the hydrocarbon releasing characteristics for pollution control and clarification of the pyrolysis mechanism [5]. Common measurement instruments and methods applied in the coal pyrolysis process detections include gas chromatography (GC), mass spectrum (MS), thermogravimetric (TG), Fourier transform infrared spectrometer (FTIR), and their combinations [6–10]. Most of these methods require pretreatment and isolation processes [11], which makes it difficult to achieve real-time and in-situ hydrocarbon measurement.

Tunable diode laser absorption spectroscopy (TDLAS) is a matured gas sensing method with the merits of high sensitivity, fast response, and low cost [12]. TDLAS has been widely used for hydrocarbon measurement in real applications like process industries [13] and combustion

diagnostics [14]. Methane and ethylene are the most common hydrocarbons detected by different lasers [15–20]. The detection of other light hydrocarbons like ethane, propene, and propane has been reported by some articles [21,22]. Several work also mentioned the laser systems for heavier hydrocarbon measurement like hydrocarbon fuel [23–25]. TDLAS can achieve real-time and in-situ measurement and thus avoid the drawbacks of the prementioned methods. However, many tunable diode lasers are only suitable for specific molecules detection due to the short spectral range and its application was therefore limited. Due to the co-existence of multiple hydrocarbons under actual conditions, the detectable species amount is a major consideration.

To overcome the shortcomings of limited wavelength range and to achieve simultaneous multispecies hydrocarbon measurement while maintaining the advantages of TDLAS, our group has proposed a hydrocarbon measurement system based on a difference frequency generation (DFG) laser [26]. The DFG laser system combines two seed laser signals through a non-linear optical medium and generates an idler beam of the difference frequency of the seed lasers. By combining the appropriate lasers, a wide spectral range in the mid-infrared region can be achieved, which is suitable for multi-species hydrocarbon measurement. With the basis of the proposed laser system discussed in the

* Corresponding author. Graduate School of Advanced Technology and Science, Tokushima University, 2-1, Minamijyanjima, Tokushima, 770-8506, Japan.

E-mail address: ydeguchi@tokushima-u.ac.jp (Y. Deguchi).

previous work [27], in this paper, the researchers present the actual applications of the system, namely the hydrocarbon measurement in the coal pyrolysis process and engine exhaust. The previous research approaches for these two applications are mainly focused on FTIR or TG/MS, and the reports on these applications using TDLAS are limited due to the drawbacks mentioned before.

2. Theory and experimental method

2.1. Theory

Direct absorption spectroscopy was used to achieve in situ measurement of gas concentrations. Gas molecules have specific absorption patterns in certain wavelengths and can be utilized to recognize their species. The TDLAS method then measures the extinction of laser light on different wavelengths. The relationship between measured light intensity and the physical properties of gas molecules are described by using the Beer-Lambert law:

$$\frac{I_\lambda}{I_0} = \exp\{-A_\lambda\} = \exp\left\{-\sum_i \left(n_i L \sum_j S_{ij}(T) G_{vij}\right)\right\} \quad (1)$$

where I_λ and I_0 represents incident and transmitted light intensity, respectively. A_λ is absorbance, n_i is the number density of species i , L is path length, S_{ij} is absorption line strength of absorption line j and G_{vij} is line broadening function.

The Beer-Lambert law can also be expressed as:

$$A = kc \quad (2)$$

where A is the absorbance, k is the absorbance coefficient and c is concentration.

By extending this formula to multiple components and wavelengths, the following equation was obtained:

$$A_i = \sum_j^n k_{ij} c_j \quad (3)$$

This equation can be transformed to its matrix form. Through matrix multiplications and setting the errors between A and kc to zero, the concentrations of components in the mixture can be obtained by using the following equation:

$$C = (K^T K)^{-1} K^T A \quad (4)$$

where C , K , and A are matrices representing concentrations of each component, pure components spectra, and the absorbance of the mixture, respectively. The absorbance k is dependent on temperature

and pressure with a nonlinear relationship. Under the conditions with different temperature and pressure, the pre-recorded spectra database at various conditions was required for the determination of concentration.

2.2. Low-temperature coal pyrolysis experimental setup

The DFG laser was a laser system consisting of an external cavity diode laser (HSL-1-10-40-ZZ-Z-T-P, Stantec co.), a DFB (distributed feedback) laser, and a DFG laser conversion module (WD-3236/3250-001-A-A-E, NTT Electronics co.). The DFB laser was placed inside the DFG module. The DFB laser was used as the pump source and the external cavity diode laser was used as the signal source to provide continuous wide spectral range scanning.

Fig. 1 displays the outline of the measurement system. The laser signal went through an absorbing cell with a 100 mm laser path, which was placed inside an electrical heating furnace. The signal detector (PVI-3TE-5-1x1-T08-wBaF2-35, VIGO System S.A.) was connected to an oscilloscope (PicoScope 5444B, Pico Technology) with a 125 MHz bandwidth. Coal powder samples made of Newlands bituminous coal powder from Australia (20 g) were placed inside a heating chamber. All the pipes and heating devices were connected to temperature controllers for temperature adjustment. Pipes were wrapped with heat isolation material for heat preservation. The orange blocks indicate the position where temperature can be adjusted. Two nitrogen gas cylinders were used, one for the transfer of gas released from coal powder and another for cell purging.

The absorbing cell was heated to 523 K and the pipes were heated to 423 K. Then the heating chamber with coal samples placed inside was heated to six discrete temperatures (373/423/473/523/573/623 K). The heating time for each temperature was 10 min. The valves of the chamber were opened when reached each discrete temperature and with the flow rate of nitrogen gas set to 50 mL/min, the gases released from the coal were carried into the absorbing cell for detection. Signals were recorded at 30-s intervals after the absorbing cell was opened and the averaging time was 200 ms. When the signal recording was finished for each temperature, the valves of the heating chamber were closed, and nitrogen gas was flowed through the absorbing cell to take away the remaining gas. The spectra recorded at 1-min count were used for analysis since the signal at this time was the strongest. The heating process was performed three times and the coal sample was replaced every time.

2.3. Engine exhaust experimental setup

The experimental setup for engine exhaust measurement was depicted in Fig. 2. A 169 cc four-stroke single-cylinder gasoline engine

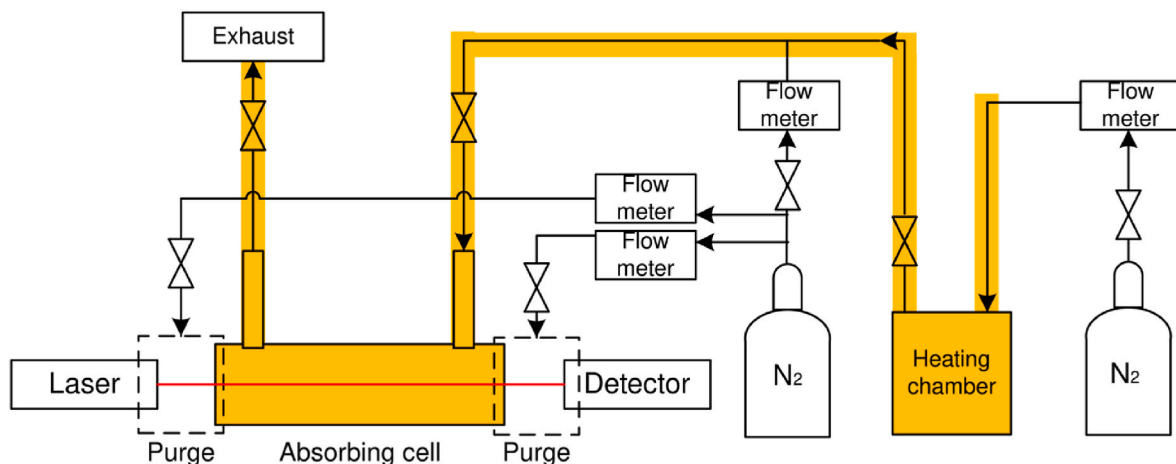


Fig. 1. Coal pyrolysis experimental setup.

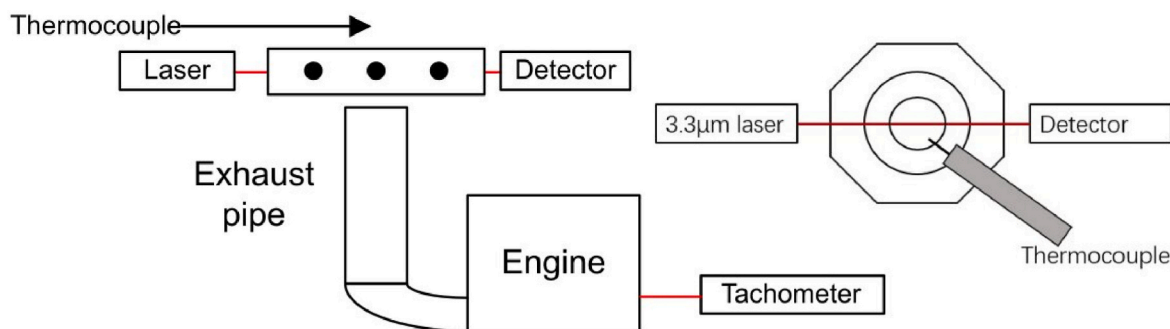


Fig. 2. Engine exhaust experimental setup.

(EX17-2BS, Fuji Heavy Industries, Inc.) was selected as the exhaust source. A tachometer (FT3406, HIOKI E.E. CORPORATION) was positioned near the engine for rotation speed measurement. The exhaust was released through an exhaust pipe with 160 mm in length, 45 mm in diameter, and 3.5 mm in thickness. A thermocouple was placed above the exhaust pipe for temperature measurement. A steel ring with drilled holes was used to fix the position of the laser path. The engine was running without any load. The recording of the spectra started from the cold start of the engine. The starting signal was triggered by the tachometer signal and set to start with the engine speed exceeding 1800 rotations per minute. The total recording time was 200 ms, which was the maximum recording time at the 6 kHz sampling rate for the oscilloscope being used.

2.4. Supplemental experiments

As a common side product of many chemical processes, water vapor acts as an interference component in hydrocarbon measurement, which was detected in both coal pyrolysis and engine exhaust experiments. It is necessary to establish a database of water vapor at different concentrations and temperatures to evaluate its influence on measurement results. The measurement system was based on the system shown in Fig. 1 by replacing the heating chamber with a water vapor generator (EA-1101, HORIBA STEC, Co.). The adjustment of water vapor concentration was achieved by changing the speed of both water vapor and nitrogen flow.

Since both actual application experiments were performed above room temperature, a database of potential pure components at different temperatures was also needed for analysis. The spectra of fifteen

hydrocarbons at four discrete temperatures were recorded above room temperature (423/523/623/723 K) at ambient pressure. Table 1 listed the measured molecules used for analysis and their experimental condition.

3. Results and discussion

3.1. Supplemental experiment results

The spectra of water vapor detected by the DFG laser system were shown in Fig. 3 (a). Multiple absorption peaks can be seen from the spectra within the detection range. The figure also showed a maximum absorbance of around 0.2 at the concentration of 80.17%. A linear fitting line was plotted in Fig. 3 (b), showing the relationship between absorbance in the highest absorption peak near 3320 nm and concentration. Compared to hydrocarbon molecules, the absorption of water is relatively weak, indicating the interference of water vapor with the spectra is also small. For example, the concentration of C_2H_6 was only 0.2% when the peak absorbance was around 0.2, which is over 400 times smaller than water vapor at a similar peak absorbance.

The spectra of C_2H_6 and C_8H_{18} at different temperatures were shown in Fig. 4, and their temperature dependence of the absorbance was checked. Two components represent the results for light hydrocarbons with sharp absorption peaks and heavy hydrocarbons without clear isolated absorption peaks, respectively. Due to the broadening of the C–H stretch bands, the absorbance of hydrocarbon molecules decreases with the increase of the temperature. In particular, for light molecules, such as CH_4 and C_2H_6 , the absorbance decrease in absorption peaks was significant. No clear shift in the wavelength for the absorption peaks was observed. For heavy molecules like C_8H_{18} , the absorption curves were smoothed out in the region where absorption is strong. The spectra of the molecules listed in Table 1 under different temperature were recorded as a database and was used for quantitative measurement. The limit of detection of each molecule was calculated by taking the SNR as 1. The blank signal spectra were used to calculate the noise level by taking its standard deviation. By comparing with the peak absorbance at certain concentrations, the limit of detection for each molecule was obtained. Both the temperature and averaging time could affect the limit of detection. The conditions listed in Table 1 were 523 K and 200 ms averaging time. Limit of detections under other conditions were calculated and used for the analysis of engine experiment and coal experiment accordingly.

3.2. Coal pyrolysis measurement

In most coal conversion processes like combustion, gasification, and liquefaction, pyrolysis is an important step [28]. Pyrolysis occurs when the temperature is up to about 973 K where light gases (such as H_2O , CH_4 , and CO), tar and char are released. When the temperature is under 673 K, the volatiles mainly comes from evaporation rather than degradation [29].

Table 1
Experimental conditions for temperature dependence of absorbance.

Species	Concentration (%)	Temperature range	Limit of detection at 523 K, 200 ms averaging time (%)
Methane (CH_4)	0.50	293–723 K	0.0030
Ethene (C_2H_4)	0.99	293–723 K	0.0247
Ethane (C_2H_6)	0.20	293–723 K	0.0036
Propene (C_3H_6)	0.98	293–723 K	0.0310
Propane (C_3H_8)	0.39	293–723 K	0.0064
<i>n</i> -Butane (C_4H_{10})	0.49	293–723 K	0.0066
<i>n</i> -Pentane (C_5H_{12})	1.26	423–723 K	0.0078
<i>n</i> -Hexane (C_6H_{14})	0.74	423–723 K	0.0079
Methylcyclohexane (C_7H_{14})	1.14	423–723 K	0.0082
<i>n</i> -Heptane (C_7H_{16})	0.99	423–723 K	0.0083
Diisobutylene (C_8H_{16})	0.93	423–723 K	0.0070
Isooctane (C_8H_{18})	0.59	423–723 K	0.0045
Benzene (C_6H_6)	2.15	423–723 K	0.0319
Toluene (C_7H_8)	2.24	423–723 K	0.0344
<i>m</i> -Xylene (C_8H_{10})	1.56	423–723 K	0.0253
Water (H_2O)	80.17	423–723 K	2.3963

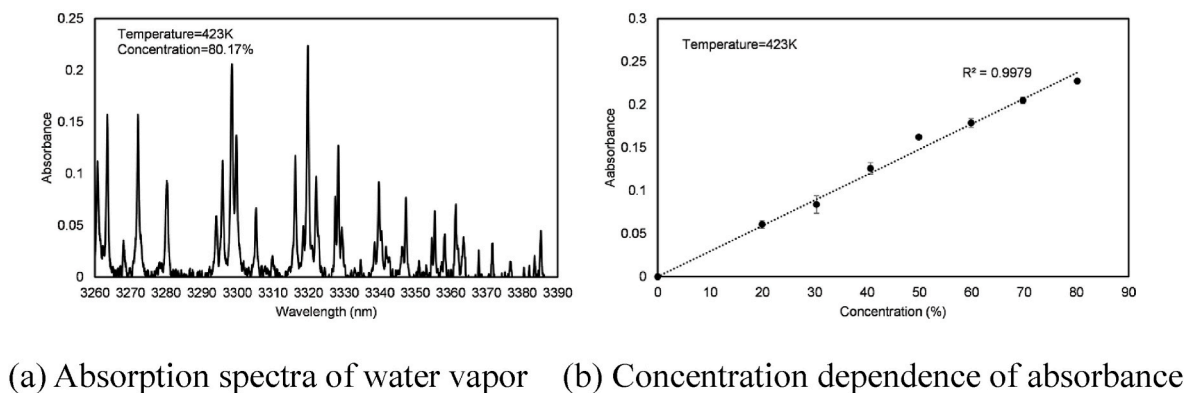
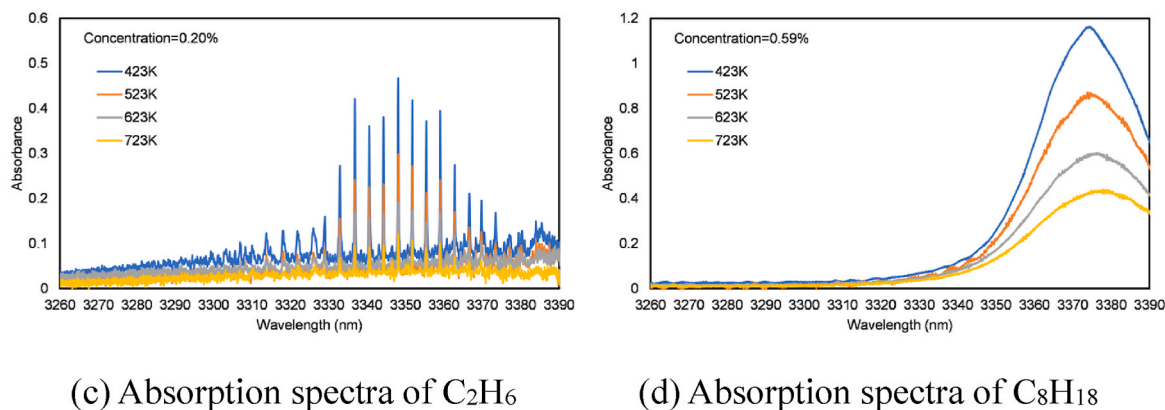


Fig. 3. Measurement results of water vapor.

Fig. 4. Temperature dependence of absorbance for C₂H₆ and C₈H₁₈.

The spectra of multiple pure hydrocarbon molecules of different classes have already been recorded before. Fig. 5 showed the spectra of all the fifteen hydrocarbons used for quantitative analysis. Light hydrocarbons (smaller than C₃) and water vapor exhibit rotation-vibration fine structure with sharp and distinguishable absorption peaks, while heavier molecules with broader absorption bands are harder to separate. The measurement results were generally identified through the comparison with the current pure hydrocarbon spectroscopic database. The spectra were recorded after the opening of the absorbing cell valves when gas flowed through the cell for 1 min. When coal samples were heated to 373 K and 423 K, only water vapor was visible from the spectra [30]. When the temperature was raised to 473 K, a small amount of absorption occurred in the 3360–3390 nm region, indicating the release of heavier aliphatic hydrocarbons. When the temperature went up to 523 K, more heavy hydrocarbons were released as the absorption in the longer wavelength continues to become bigger. At the temperature above 573 K, clear absorption peaks of CH₄ and C₂H₆ were found, as shown in Fig. 6 (e) and Fig. 6 (f). In general, the aromatic hydrocarbons undergo absorption in the wavelength region smaller than 3320 nm, which was also observed when the coal sample was heated to over 573 K.

For quantitative analysis of the results, the least-squares fitting of the spectra was performed. And this method has already been used by our group for hydrocarbon mixture separation under given conditions, and its reliability has been proved. Based on the measured pure hydrocarbon spectra at given concentration and temperature, the concentration of each potential component within the mixture was calculated using the method mentioned in section 2.1. Least-squares fittings were performed at temperatures higher than 473 K. The measured and fitted spectra at 623 K were shown in Fig. 7. The R² value was used to assess the quality

between the measured data and the model. If the R² value is close to 1, it indicates that the linear regression of the data is in good condition with small variances. The experiments were performed three times and the averaged R² value of the fitting results at 623 K was 0.994, showing good fitting performance. The minimum R² value of 0.939 appeared at 523 K. The bigger absorbance may lead to better fitting results due to the smaller influence of noise.

By using the least-squares fitting method, the concentration of each component in the mixture was calculated and the hydrocarbons above the limit of detection were shown in Fig. 8. Considering the water vapor as an interference component, its concentration was not included in the figure. Based on the calculation results, eleven hydrocarbons were above the limit of detection. The concentrations of C₂H₄, C₂H₆, and C₈H₁₆ were rather small compared with other hydrocarbons. The concentration of C₂H₄ was above the limit of detection only at 623 K, and the C₂H₆ was detectable when the temperature rose to 573 K. The concentration of C₈H₁₆ was relatively small among all three temperatures. The concentrations of all other components increase with the increase of the temperature. The fitting results were consistent with the qualitative identification results. Coal pyrolysis is a complicated process with many gaseous and oil products. Though common approaches for hydrocarbon measurement using FTIR can cover broader wavelength from near-infrared to mid-infrared region, the resolution is lower, and the devices are less compact. According to previous reports, the released gaseous hydrocarbons during the pyrolysis process range from C₁–C₆ [7, 31,32], heavier hydrocarbons were usually not separated in the references. The current fitting result demonstrated the approach, and better results could be achieved if the database were enlarged by more hydrocarbon spectra.

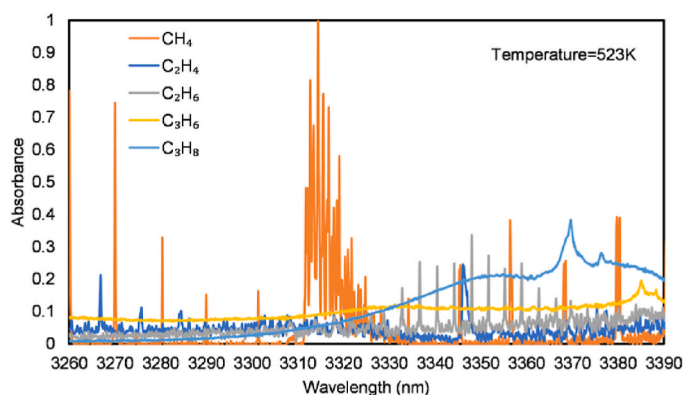
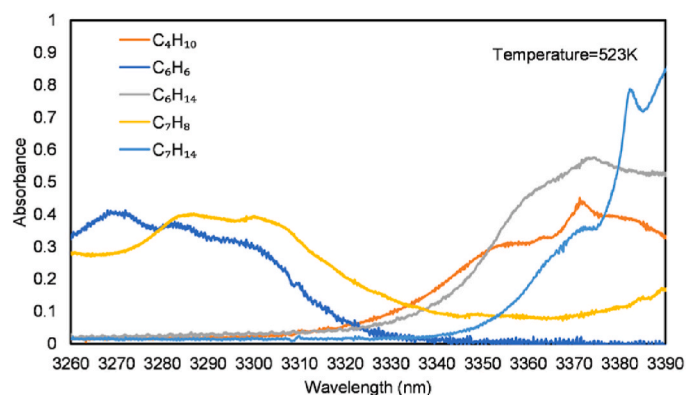
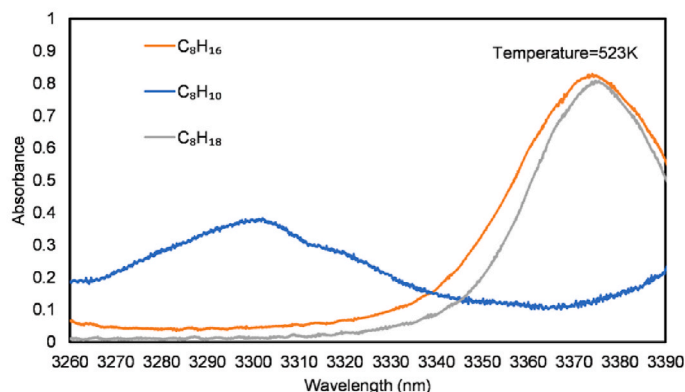
(a) Spectra of C₁-C₃ hydrocarbons(b) Spectra of C₄-C₇ hydrocarbons(c) Spectra of C₈ hydrocarbons

Fig. 5. Spectra of pure hydrocarbon spectra at 523 K.

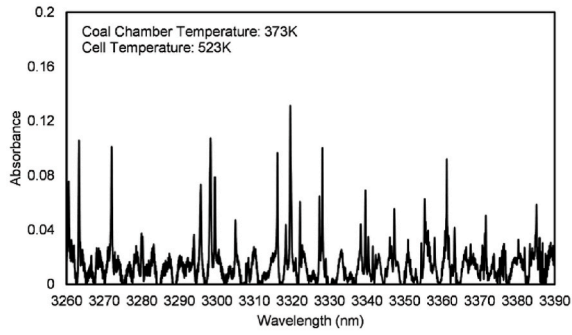
3.3. Engine exhaust measurement

Hydrocarbon is a common material that can be detected in engine exhaust from both unburned fuel and finished combustion reactions. The components of the engine exhaust vary with different engine types, ignitions, fuel types, test methods, etc. [33,34] Despite the variations of conditions, most components are common groups, such as alkanes, alkenes, and aromatics, which are identical to our current database. The engine employed in this experiment was a four-stroke engine, which means that the release of the exhaust is not consistent. The rotation speed and the thermocouple measurement result were displayed in Fig. 9. The sampling period of the tachometer was 80 ms, which caused a sudden drop in rotation speed during the measurement. Considering the rotation speed of the engine, the recorded spectra were averaged every 20 ms for analysis.

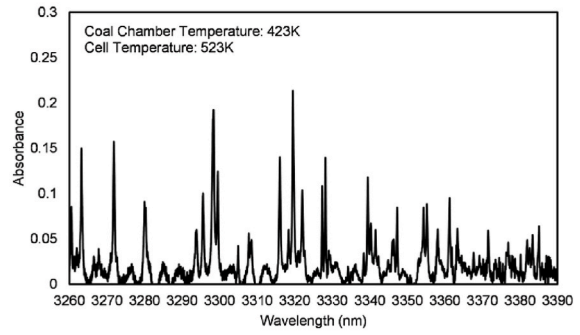
The averaged spectra during four different averaging periods were shown in Fig. 10, which illustrates the change of absorbance. It can be seen from Fig. 10 (a) that the absorption at wavelength >3330 nm was strong which indicates the occurrence of heavy aliphatic hydrocarbons. While minor absorption in 3260–3330 nm could be caused by aromatic hydrocarbons. Fig. 10 (b) illustrated a weaker absorption spectrum with almost no absorption in the region from 3260 to 3300 nm, which means that the signal was recorded between the interval of exhaust release. The absorption pattern shown in Fig. 10(c) is similar to those in Fig. 10(a) and (b), and sharp absorption peaks for CH₄ can be identified. For quantitative analysis, the least-squares fitting was also performed. In addition to CH₄, six other hydrocarbons were identified from the fitting

results. Fitted and measured spectra at the time interval from 180 ms to 200 ms were shown in Fig. 11. For all the periods, the R² values between the fitting results and measured spectra were larger than 0.970, indicating good fitting results. The deviation was larger than the results of coal measurement, which could be caused by the temperature difference between measured spectra and pure spectra. Another factor lies in the shorter averaging time which enlarged the noise level. Fig. 12 depicted the variation of the concentration of these hydrocarbons with time. The main components detected from the engine exhaust were aliphatic hydrocarbons. The concentration of C₂H₄ was above the limit of detection only within the first 0–20 ms, while the concentration of other components all fluctuates at different time intervals, indicating the capability of the system on capturing the change of hydrocarbon release in engine emissions.

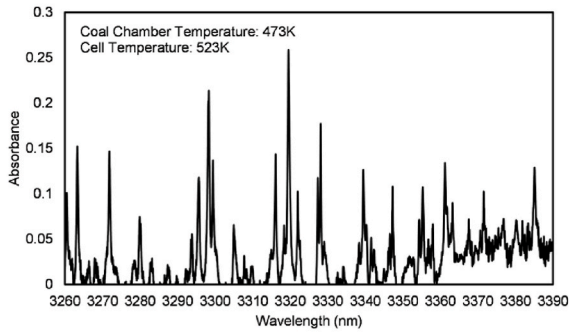
Different hydrocarbons were analyzed in the previous research by using FTIR [35], but since heavier hydrocarbon molecules share a close similarity in absorption band shapes, only light molecules were separated. More detailed profiles for different components were achieved by using other methods like gas chromatography [36]. However, the devices are usually heavier, more expensive, and hard to achieve real-time measurement. Based on the comparison with the results of previous reports, the number of light hydrocarbons (like methane and ethylene) is smaller than that of the heavier molecules. Despite the different experiment setups, the spectra recording of this research is limited to a short period after a cold start, therefore, the exhaust includes more unburned hydrocarbons rather than burned products.



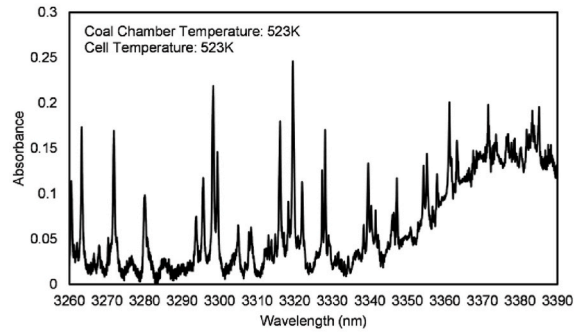
(a) Absorption spectra at 373K



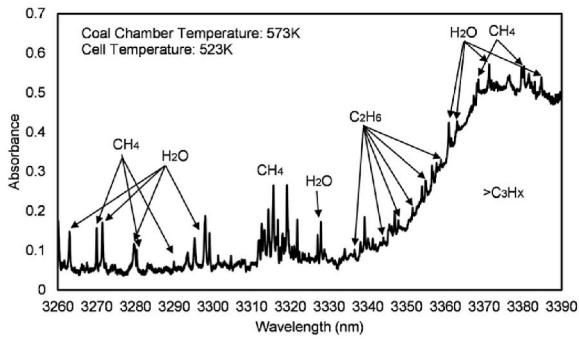
(b) Absorption spectra at 423K



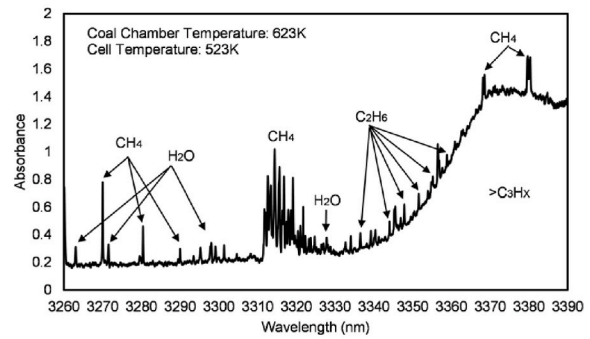
(c) Absorption spectra at 473K



(d) Absorption spectra at 523K



(e) Absorption spectra at 573K



(f) Absorption spectra at 623K

Fig. 6. Absorption spectra of coal pyrolysis at different temperature.

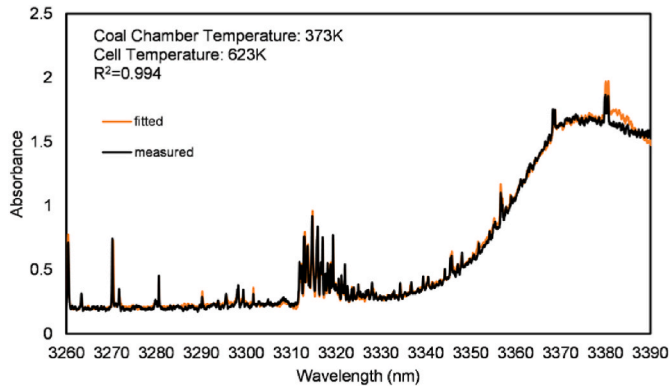


Fig. 7. Fitted and measured results at 623 K.

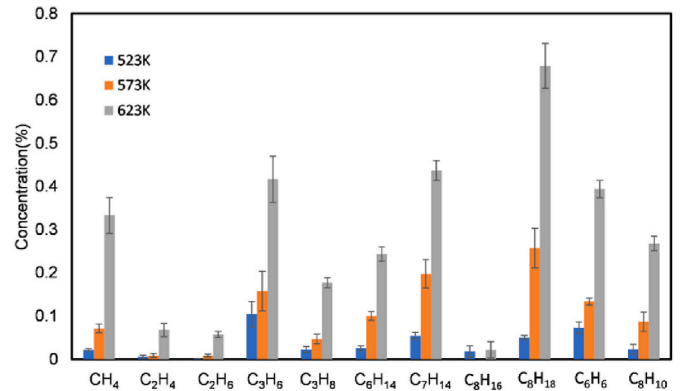


Fig. 8. Calculated results for hydrocarbons above limit of detection.

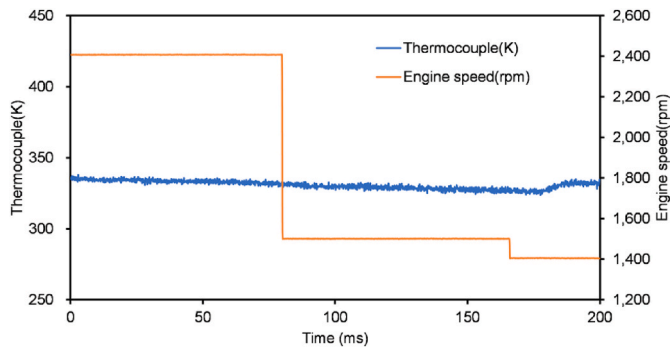


Fig. 9. Rotation speed of engine and thermocouple result.

4. Conclusion

This study demonstrated the applications of a DFG laser system in hydrocarbon measurement. The hydrocarbons released from the coal pyrolysis process and engine exhaust were detected and the recorded spectra were analyzed. Conclusions are drawn as follows.

- (1) Coal powder samples were heated from 373 K to 623 K at a constant interval of 50 K. The release of aliphatic hydrocarbon gas started above 473 K, and small hydrocarbon molecules, such as CH₄ and C₂H₆ were detected above 523 K. Besides, the aromatic hydrocarbons appeared when the temperature was over 573 K. Fifteen pure hydrocarbons were heated to four discrete temperatures between 423 K and 723 K and the spectra were recorded as a database. Based on the database, least-squares fitting was performed, with a minimum R² value of 0.939, showing a small variance between fitted and measured spectra. Moreover, nine different hydrocarbon molecules above the limit of detection were identified quantitatively.

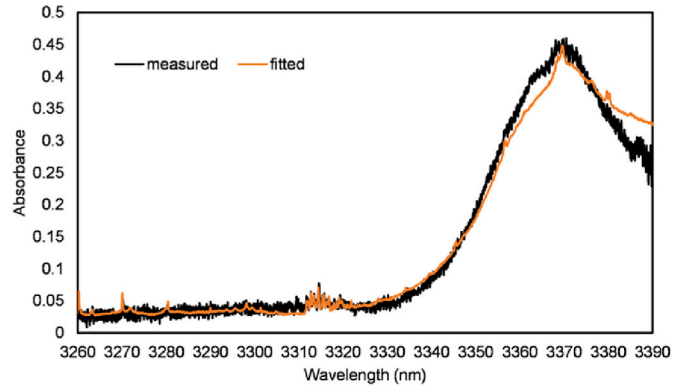


Fig. 11. Fitted and measured results from 180 to 200 ms.

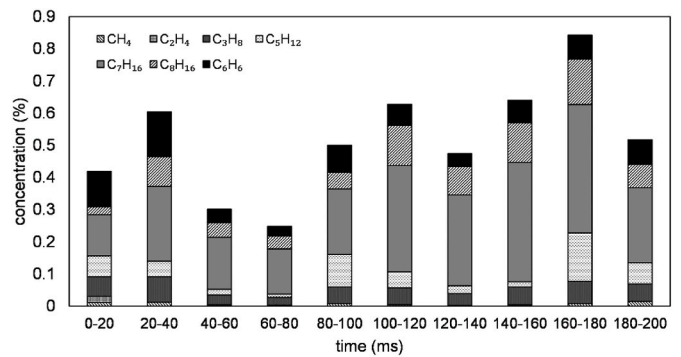
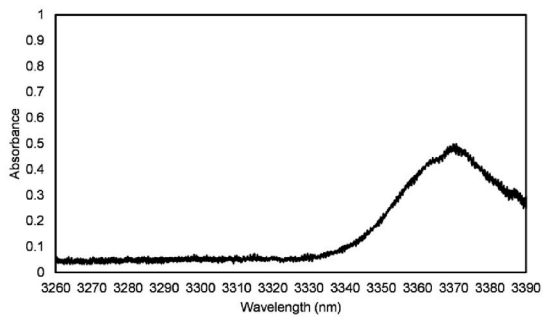
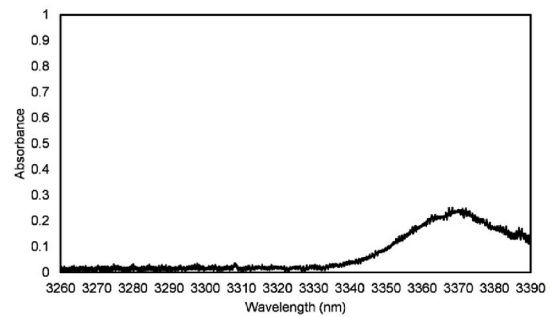


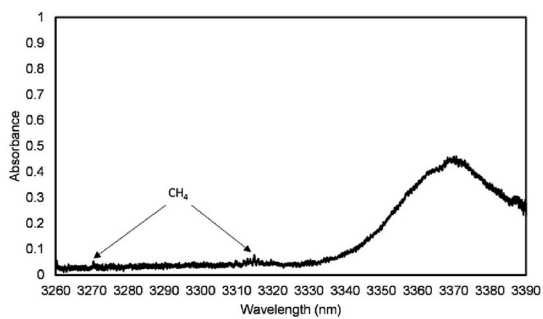
Fig. 12. Calculated concentration of hydrocarbons above limit of detection at different time periods.



(a) Absorption spectra at 20-40ms



(b) Absorption spectra at 60-80ms



(c) Absorption spectra at 180-200ms (d) Absorption spectra at 180-200ms (enlarged)

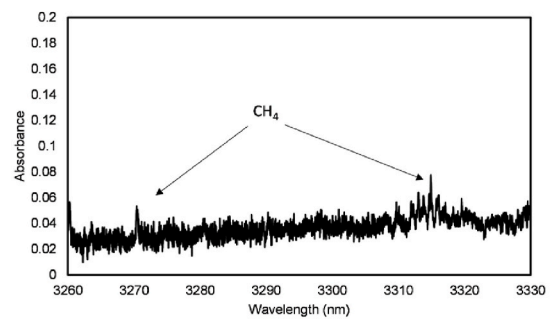


Fig. 10. Absorption spectra of engine exhaust at different time periods.

(2) Engine exhaust was detected, and the spectra were recorded, which were analyzed at an interval of 20 ms based on the rotation speed of the engine. The change in absorbance was observed among different time intervals, proving the capability of the laser system on real-time measurement. The spectra were also analyzed by using the least-squares fitting method and seven hydrocarbon molecules were identified above the limit of detection.

It was proved by the two experiments that the proposed laser system was available for the detection of multiple hydrocarbons simultaneously in actual situations. Moreover, further study is necessary to acquire the spectra of more hydrocarbons that may exist in the processes being measured.

Author statement

Qiming Wang: Methodology, Investigation, Formal analysis, Data Curation, Writing – Original Draft. Zhenzhen Wang: Writing - Review & Editing. Takahiro Kamimoto: Investigation, Resources, Yoshihiro Deguchi: Methodology, Supervision. Du Wen: Data Curation, Writing - Review & Editing. Daichi Takahara: Writing - Investigation, Review & Editing.

Declaration of competing interest

The authors declare that they have no known competing financial interests or personal relationships that could have appeared to influence the work reported in this paper.

References

- J. Liu, X. Jiang, J. Shen, H. Zhang, Pyrolysis of superfine pulverized coal. Part 1. Mechanisms of methane formation, *Energy Convers. Manag.* 87 (2014) 1027–1038, <https://doi.org/10.1016/j.enconman.2014.07.053>.
- M.A. Serio, D.G. Hamblen, J.R. Markham, P.R. Solomon, Kinetics of volatile product evolution in coal pyrolysis: experiment and theory, *Energy Fuel*. 1 (2) (1987) 138–152, <https://doi.org/10.1021/ef00002a002>.
- E. Torres, et al., 4-E (environmental, economic, energetic and exergetic) analysis of slow pyrolysis of lignocellulosic waste, *Renew. Energy* 162 (2020) 296–307, <https://doi.org/10.1016/j.renene.2020.07.147>.
- P. Sette, A. Fernandez, J. Soria, R. Rodriguez, D. Salvatori, G. Mazza, Integral valorization of fruit waste from wine and cider industries, *J. Clean. Prod.* 242 (2020), <https://doi.org/10.1016/j.jclepro.2019.118486>.
- L.R. Ortiz, E. Torres, D. Zalazar, H. Zhang, R. Rodriguez, G. Mazza, Influence of pyrolysis temperature and bio-waste composition on biochar characteristics, *Renew. Energy* 155 (2020) 837–847, <https://doi.org/10.1016/j.renene.2020.03.181>.
- Z. Niu, G. Liu, H. Yin, D. Wu, C. Zhou, Investigation of mechanism and kinetics of non-isothermal low temperature pyrolysis of perhydrous bituminous coal by in-situ FTIR, *Fuel* 172 (2016) 1–10, <https://doi.org/10.1016/j.fuel.2016.01.007>.
- M. Wang, Z. Li, W. Huang, J. Yang, H. Xue, Coal pyrolysis characteristics by TG-MS and its late gas generation potential, *Fuel* 156 (2015) 243–253, <https://doi.org/10.1016/j.fuel.2015.04.055>.
- Q. He, K. Wan, A. Hoadley, H. Yeasmin, Z. Miao, TG-GC-MS study of volatile products from Shengli lignite pyrolysis, *Fuel* 156 (April) (2015) 121–128, <https://doi.org/10.1016/j.fuel.2015.04.043>.
- A. Arenillas, C. Pevida, F. Rubiera, R. García, J.J. Pis, Characterisation of model compounds and a synthetic coal by TG/MS/FTIR to represent the pyrolysis behaviour of coal, *J. Anal. Appl. Pyrolysis* 71 (2) (2004) 747–763, <https://doi.org/10.1016/j.jaap.2003.10.005>.
- A. Saffe, A. Fernandez, M. Echegaray, G. Mazza, R. Rodriguez, Pyrolysis kinetics of regional agro-industrial wastes using isoconversional methods, *Biofuels* 10 (2) (2019) 245–257, <https://doi.org/10.1080/17597269.2017.1316144>.
- L. Jia, J. Weng, Y. Wang, S. Sun, Z. Zhou, F. Qi, Online analysis of volatile products from bituminous coal pyrolysis with synchrotron vacuum ultraviolet photoionization mass spectrometry, *Energy Fuel*. 27 (2) (Feb. 2013) 694–701, <https://doi.org/10.1021/ef301670y>.
- Y. Deguchi, *Industrial Applications of Laser Diagnostics*, CRC Press, 2016.
- M. Lackner, Tunable diode laser absorption spectroscopy (TDLAS) in the process industries - a review, *Rev. Chem. Eng.* 23 (2) (2007) 65–147, <https://doi.org/10.1515/REVCE.2007.23.2.65>.
- M.A. Bolshov, Y.A. Kuritsyn, Y.V. Romanovskii, Tunable diode laser spectroscopy as a technique for combustion diagnostics, *Spectrochim. Acta Part B At. Spectrosc.* 106 (2015) 45–66, <https://doi.org/10.1016/j.sab.2015.01.010>.
- R. Sur, S. Wang, K. Sun, D.F. Davidson, J.B. Jeffries, R.K. Hanson, High-sensitivity interference-free diagnostic for measurement of methane in shock tubes, *J. Quant. Spectrosc. Radiat. Transf.* 156 (2015) 80–87, <https://doi.org/10.1016/j.jqsrt.2015.01.023>.
- C.S. Goldenstein, R.M. Spearrin, J.B. Jeffries, R.K. Hanson, Infrared laser-absorption sensing for combustion gases, *Prog. Energy Combust. Sci.* 60 (2017) 132–176, <https://doi.org/10.1016/j.pecs.2016.12.002>.
- B. Koroglu, S. Neupane, O. Pryor, R.E. Peale, S.S. Vasu, High temperature infrared absorption cross sections of methane near 3.4 μm in Ar and CO₂ mixtures, *J. Quant. Spectrosc. Radiat. Transf.* 206 (2018) 36–45, <https://doi.org/10.1016/j.jqsrt.2017.11.003>.
- T. Zhang, G. Zhang, X. Liu, G. Gao, T. Cai, A TDLAS sensor for simultaneous measurement of temperature and C₂H₄ concentration using a differential absorption scheme at high temperature, *Front. Physiol.* 8 (2020) 1–7, <https://doi.org/10.3389/fphy.2020.00044>, March.
- G. Gao, T. Zhang, G. Zhang, X. Liu, T. Cai, Simultaneous and interference-free measurements of temperature and C₂H₄ concentration using a single tunable diode laser at 162 μm , *Opt Express* 27 (13) (2019) 17887, <https://doi.org/10.1364/oe.27.017887>.
- K. Tanaka, K. Akishima, M. Sekita, K. Tonokura, M. Konno, Measurement of ethylene in combustion exhaust using a 3.3- μm distributed feedback interband cascade laser with wavelength modulation spectroscopy, *Appl. Phys. B Laser Opt.* 123 (8) (2017) 1–8, <https://doi.org/10.1007/s00340-017-6798-4>.
- C. Li, L. Dong, C. Zheng, F.K. Tittel, Compact TDLAS based optical sensor for ppb-level ethane detection by use of a 3.34 μm room-temperature CW interband cascade laser, *Sensor. Actuator. B Chem.* 232 (2016) 188–194, <https://doi.org/10.1016/j.snb.2016.03.141>.
- Y. Wang, T. Jiang, Y. Wei, T. Liu, T. Sun, K.T.V. Grattan, TDLAS Detection of propane and butane gas over the near-infrared wavelength range from 1678nm to 1686nm, *J. Phys. Conf. Ser.* 1065 (2018) 25, <https://doi.org/10.1088/1742-6596/1065/25/252006>.
- A.E. Klingbeil, J.B. Jeffries, R.K. Hanson, Tunable mid-IR laser absorption sensor for time-resolved hydrocarbon fuel measurements, *Proc. Combust. Inst.* 31 I (1) (2007) 807–815, <https://doi.org/10.1016/j.proci.2006.07.228>.
- J.M. Porter, J.B. Jeffries, R.K. Hanson, Mid-infrared absorption measurements of liquid hydrocarbon fuels near 3.4 μm , *J. Quant. Spectrosc. Radiat. Transf.* 110 (18) (2009) 2135–2147, <https://doi.org/10.1016/j.jqsrt.2009.05.017>.
- S. Wang, T. Parise, S.E. Johnson, D.F. Davidson, R.K. Hanson, A new diagnostic for hydrocarbon fuels using 3.41- μm diode laser absorption, *Combust. Flame* 186 (2017) 129–139, <https://doi.org/10.1016/j.combustflame.2017.07.026>.
- D. Richter, A. Fried, P. Weibring, Difference frequency generation laser based spectrometers, *Laser Photon. Rev.* 3 (4) (2009) 343–354, <https://doi.org/10.1002/lpor.200810048>.
- Q. Wang, et al., Multi-species hydrocarbon measurement using TDLAS with a wide scanning range DFG laser, *Spectrochim. Acta Part A Mol. Biomol. Spectrosc.* 265 (2022) 120333, <https://doi.org/10.1016/j.saa.2021.120333>.
- P. Khare, B.P. Baruah, P.G. Rao, Application of chemometrics to study the kinetics of coal pyrolysis: a novel approach, *Fuel* 90 (11) (2011) 3299–3305, <https://doi.org/10.1016/j.fuel.2011.05.017>.
- W.R. Ladner, The products of coal pyrolysis: properties, conversion and reactivity, *Fuel Process. Technol.* 20 (1988) 207–222, [https://doi.org/10.1016/0378-3820\(88\)90021-5](https://doi.org/10.1016/0378-3820(88)90021-5).
- A. Saffe, A. Fernandez, G. Mazza, R. Rodriguez, Prediction of regional agro-industrial wastes characteristics by thermogravimetric analysis to obtain bioenergy using thermal process, *Energy Explor. Exploit.* 37 (1) (2019) 544–557, <https://doi.org/10.1177/0144598718793908>.
- L. Luo, J. Liu, H. Zhang, J. Ma, X. Wang, X. Jiang, TG-MS-FTIR study on pyrolysis behavior of superfine pulverized coal, *J. Anal. Appl. Pyrolysis* 128 (2017) 64–74.
- F. Han, A. Meng, Q. Li, Y. Zhang, Thermal decomposition and evolved gas analysis (TG-MS) of lignite coals from Southwest China, *J. Energy Inst.* 89 (1) (2016) 94–100.
- W. Hong-li, et al., Volatile organic compounds (VOCs) source profiles of on-road vehicle emissions in China, *Sci. Total Environ.* 607 (608) (2017) 253–261, <https://doi.org/10.1016/j.scitotenv.2017.07.001>.
- D. Albaladejo-Hernández, F.V. García, J. Hernández-Grau, Influence of catalyst, exhaust systems and ECU configurations on the motorcycle pollutant emissions, *Results Eng.* 5 (2020) 100080, <https://doi.org/10.1016/j.rineng.2019.100080>.
- C.A. Gierczak, L.L. Kralik, A. Mauti, A.L. Harwell, M.M. Maricq, Measuring NMHC and NMOG emissions from motor vehicles via FTIR spectroscopy, *Atmos. Environ.* 150 (x) (2017) 425–433, <https://doi.org/10.1016/j.atmosenv.2016.11.038>.
- C.A. Jemna, P.R. Shore, K.A. Widdicombe, Analysis of C₁-C₁₆ hydrocarbons using dual-column capillary GC: application to exhaust emissions from passenger car and motorcycle engines, *J. Chromatogr. Sci.* 33 (1) (1995) 34–48.